

STUDY OF EFFECTS OF A BERM ON THE STABILITY  
ON ROCKFILL DAMS DURING EARTHQUAKES

by  
S. Okamoto<sup>I</sup>, C. Tamura<sup>II</sup>, T. Ohmachi<sup>III</sup> and K. Kato<sup>IV</sup>

SYNOPSIS

Vibration failure experiments and numerical analyses of large-sized two-dimensional models of rockfill dams are carried out to study stabilities of dams of this type during earthquake. The paper describes the results of vibration failure experiments on models of dams each provided with a berm on one of its slopes and the results of numerical analyses of influences of provision of a berm on stress distribution inside a dam body.

I. VIBRATION FAILURE EXPERIMENTS ON LARGE-SIZED MODELS

I-1. Models

Two-dimensional large-sized models 1.4 m in height were constructed on a large shaking table and were vibrated to failure by sinusoidal wave-forms of about 2 Hz increasing amplitude in one direction horizontally. The material for the models described in this paper was  $\phi 206$ -cm round gravel (mixture of quartzite, sandstone and limestone, specific gravity 2.56) with unit weight of 1.6 ton/m<sup>3</sup> and angle of repose of 40.4°. The models were constructed on the steel plate of the shaking table and were secured against sliding by means of steel channels. In order to ascertain deformations inside the dam bodies, colored pieces of the material for the models were embedded in columnar form, besides which accelerometers and strain gages were installed, while colored pieces were also lined up on the surfaces to serve as reference points for checking deformation. A berm 50-cm wide was provided at a height of either 70 cm or 90 cm from the foundation.

I-2. Results of Experiments

Thirty sec to 1 min were required from start to end of shaking in the experiments. Since the vibration frequency applied was extremely low compared with the fundamental frequency, the acceleration of an entire dam body was more or less constant until immediately before crumbling of slopes. Fig. 1 shows the surface deformation after testing in case of no water and the numerals accompanying the arrows indicate distances in terms of cm that surface reference points moved in the directions of the arrows. Vibrations were applied at 3.4 Hz in this experiment, and when approximately 0.42 g was reached, crumbling occurred below the shoulder of the berm, followed by crumbling at the mid-height portion of the slope above the berm. The acceleration was stepped up further to approximately 0.49 g and the degree of crumbling was increased. Partial sliding as seen in visual inspection was judged as constituting crumbling.

Fig. 2 gives the results of similar experiments made with a model having a berm at a height of 90 cm on impounding water. The straight

- 
- I. Professor Emeritus, University of Tokyo, President, Saitama University  
II. Professor, Institute of Industrial Science, University of Tokyo  
III. Research Engineer, Electric Power Development Co., Ltd.  
IV. Research Fellow, Institute of Industrial Science, University of Tokyo




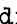
broken line drawn from the crest in the figure is a thin rubber membrane for water cut-off, the black dots in a row are colored particles for reference points, while  and  indicate accelerometers. The waveform of the No. 2 accelerometer at mid-height of the lower slope first starts to be distorted at acceleration of 0.20 g, and the waveform of the No. 5 accelerometer at mid-height of the upper slope begins to be distorted at 0.23 g. The maximum acceleration reaches 0.35 g. The broken line along the slopes indicates the surface of the dam after the experiment. According to experiments conducted up to this time, the acceleration at which crumbling occurs when water has been impounded is about 60% that when empty.

Fig. 3 shows the results of similar experiments with a model having straight line slopes of 1:1.8. The bold solid line indicates the surface of the dam while  and  marks indicate the post-experiment locations of colored particles which had been embedded in columnar form for reference. The maximum acceleration in this experiment was 0.43 g, and it can be seen that the state of failure was severe compared with the case of Fig. 1 (maximum acceleration 0.49 g).

Three or more experiments were conducted for each type of model in this study and there was good agreement of the results for each of the types. The following were observed as results of the experiments:

- 1) The effect of berm-height for slope stability is better for 90 cm than for 70 cm.
- 2) For both berm-heights of 70 cm and 90 cm, crumbling first occurs below the shoulders of berms followed by crumbling of upper portion slopes.
- 3) For slopes of identical gradients, there must be greater acceleration in case there is a berm in order for crumbling to be produced.
- 4) Whereas a slope with no berm shows crumbling of the entire slope, the berm portion of a slope with a berm is stable and does not readily crumble so that it is difficult for all-out crumbling to occur.
- 5) Crumbling of slopes above and below a berm is of smaller scale compared with when there is no berm.

## II. STUDY BY NUMERICAL ANALYSIS

Since the accelerations inside dam bodies in these experiments were constant and equal to the acceleration of the shaking table until immediately before crumbling, the stress values within the dam bodies were computed by the finite element method based on elastic theory using the seismic coefficient method. Fig. 4 shows the principal stress distribution in case of a trapezoidal cross section with the gradients of both upstream and downstream slopes the same at 1:1.8 considering the foundation as a rigid body. In calculations of stresses, that the dam material had extremely little or no tensile strength was taken into consideration, the method of giving anisotropic properties to the material was taken by which when a principal tensile stress was produced the modulus of elasticity in its direction would be lowered by the following equation:

$$E' = E / (1 - K\sigma)$$

where E is modulus of elasticity for compressive stress,  $\sigma$  is tensile stress (compressive stress positive), E' is modulus of elasticity for

tensile stress, and  $K$  is an optional positive number,  $K = 0$  in case of  $\sigma \geq 0$ . In case of horizontal seismic coefficient of 0.2, the portion surrounded by the left-side slope,  $K = 1$  in this case, is a zone where tensile stresses are produced along the slope, and these tensile stresses are extremely small. This zone has a fairly small area compared with the case when  $E$  is not changed, and it is found that stress distribution at the opposite side (vicinity of compression side) is barely influenced by development of this zone. When subjected to vibration load, the slopes alternately demonstrate states of tensile stress (loosening state) and compressive stress and this is important in considering slope stability. Fig. 5 shows the principal stress distribution when a slope with a berm has gone into a state of compressive stress. Unlike the stress distribution of the right-hand slope of Fig. 4, because of the existence of a berm, the size and direction of the principal stress are changed at the portion where the berm is provided. The change is to a distribution just as if the flow of principal stress were to run down along the vicinity of the berm in a form that a portion indicating a high stress intensity is enveloped inside the berm part.

As reported previously, crumbling of a slope may be explained by assumption of a friction system, while it has been recognized that crumbling can occur in case the maximum angle of inclination of stress at the slope portion on the compression side exceeds a certain value and in addition spreads over a wide range along the slope. Figs. 6 and 7 shows the distributions of sine values of maximum angles of inclination of stresses for a trapezoidal cross section and a cross section with a berm. The frictional angle at the time of crumbling of a slope as determined by visual inspection is  $50^\circ$  and the sine value of this is 0.75. In Fig. 6, when seismic coefficient becomes larger than 0.3, the surface portion of the slope on the compression side and a fairly large portion toward the bottom become zones exceeding this value. When the seismic coefficient approaches 0.4 the entire surface layer of the slope exceeds 0.75, and it is seen that overall crumbling will occur. Meanwhile, in Fig. 7, in case of seismic coefficients of 0.3 and 0.4 there are zones produced at the slopes above and below the berm where this value is exceeded, but at the upper slope the zone is small and disappears before reaching down to the berm. As for the lower slope, the zone is smaller than for the case of Fig. 6. Furthermore, immediately under the berm there is a broad zone where the value is extremely small and which can be considered as preventing the upper and lower slopes joining together in crumbling.

Next, in Figs. 8 and 9, when frictional angle is  $50^\circ$  and cohesion is ignored, whether sliding is possible at each point according to the stress condition is indicated, as well as the direction in case sliding is possible taking only a portion of the slope. In these figures, points where fan shapes are drawn can slide, and moreover, the directions in which they can slide are in the ranges of the fan shapes. From these figures it can be seen that the slope below the berm is more susceptible to sliding than the slope above, that the surface of the upper slope at seismic coefficient of 0.3 will show almost no sliding or sliding at an extremely small portion, that the surface layer as a whole slides when seismic coefficient becomes 0.4, and further, that the berm portion does not slide and is stable. Fig. 9 indicates that when there is no berm the entire slope may slide down even at seismic coefficient of 0.3.

### III. CONCLUSION

It has been shown in the above that the crumbling phenomena of slopes in experiments can be interpreted fairly well through consideration of the stabilities during earthquake of slopes with berms based on numerical studies. Consequently, it will be possible to rationally design locations and widths of berms through such numerical analyses.

### ACKNOWLEDGEMENTS

The authors wish to express their gratitude to Mr. K. Ono, Mr. H. Katayama, Mr. K. G. Bhatia and the Tokyo Electric Power Co., Inc. for their splendid cooperation in carrying out this study.

### BIBLIOGRAPHY

- 1) S. Okamoto, C. Tamura, K. Kato and T. Ohmachi: "A Study on the Dynamic Stability of Rock-fill Dam during Earthquakes Based on Vibration Failure Tests of Models," 5th Symposium on Earthquake Engineering, Roorkee, India, 1974.

Fig.1 Profile of Model Dam with a Berm after Vibration Failure Test. (empty condition)

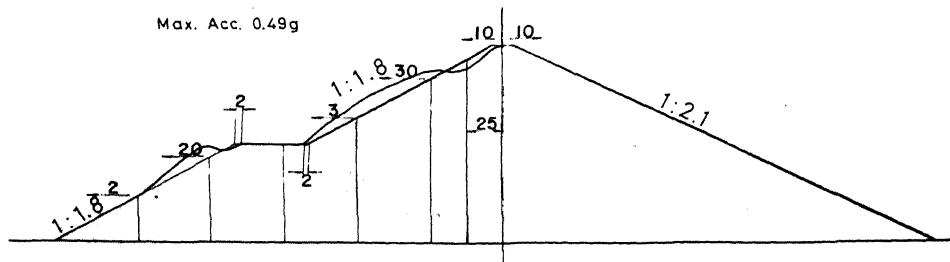


Fig.2 Profile of Model Dam with a Berm after Vibration Failure Test. (full reservoir condition)

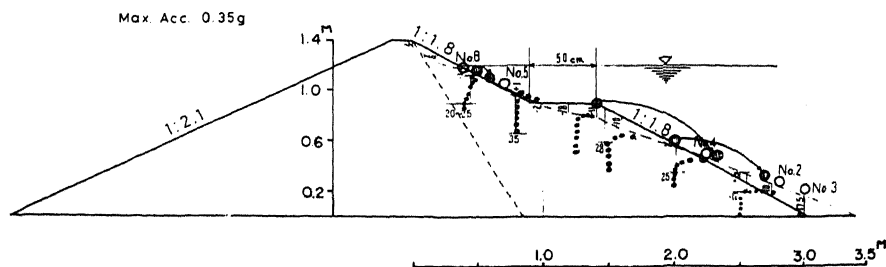


Fig.3 Profile of Model Dam after Vibration Failure Test.  
(empty condition)

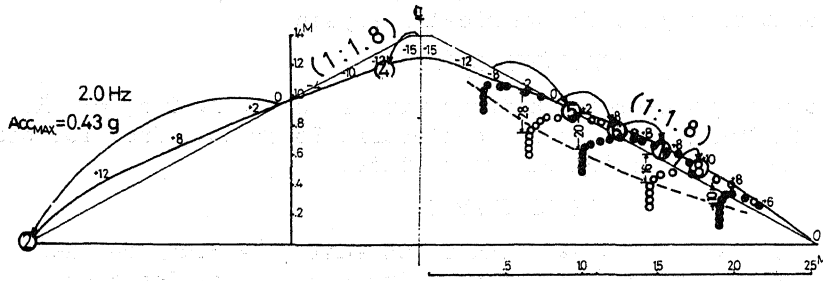


Fig.4 Diagram of Principal Stress.

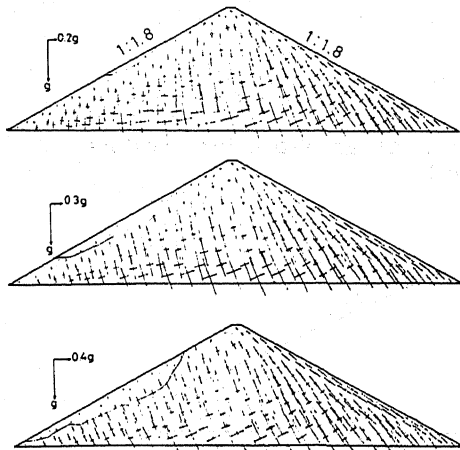


Fig.5 Diagram of Principal Stress.

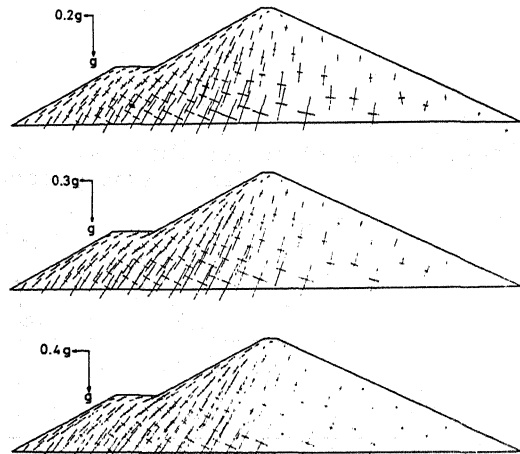


Fig.6 Contour Line of Sine Value to Max. Angle of Inclination of Stress.

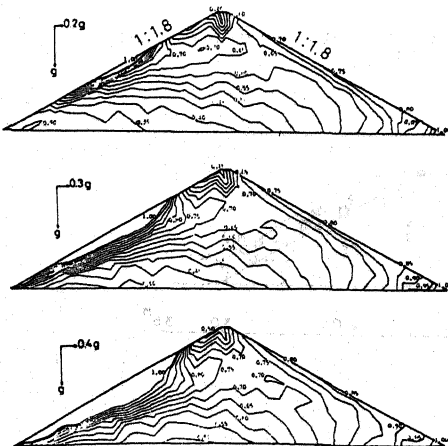
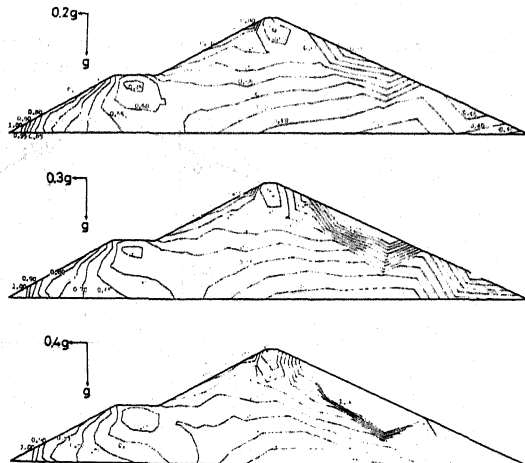


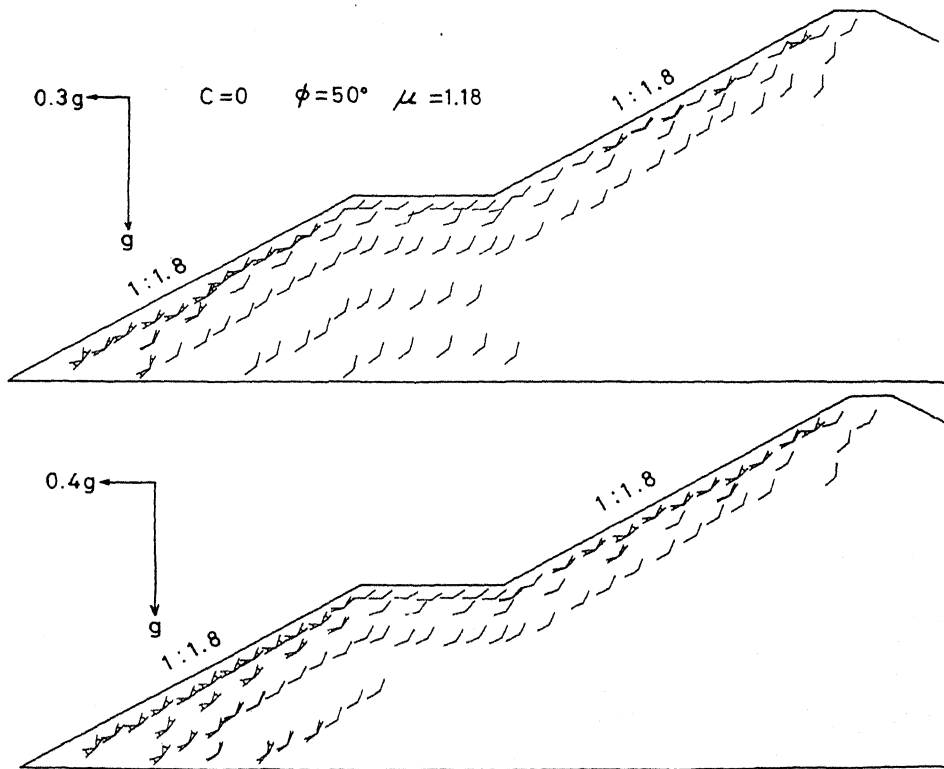


Fig.7 Contour Line of Sine Value to Max. Angle of Inclination of Stress.





**Fig.8 Predicted Slip Directions**

-  Slips occur in the calculation.  
Slip direction exist in fan zone.
-  No slip occur in the calculation.  
Lines show possible slip directions.



**Fig.9 Predicted Slip Directions**

-  Slips occur in the calculation.  
Slip direction exist in fan zone.
-  No slip occur in the calculation.  
Lines show possible slip directions.

